Research Paper

Influence of matrix effects by inorganic ions in single-cell direct mass spectrometry

Yoshihiro Kato[1], Shinobu Kudoh[2], Eiji Sugiyama[1], Iwao Sakane[3], Naohiro Tsuyama[4], Toshimasa Toyo'oka[1], Kenichiro Todoroki[1], Hajime Mizuno[1,5]*

[1]Laboratory of Analytical and Bio-Analytical Chemistry, School of Pharmaceutical Sciences, University of Shizuoka, 52−1 Yada, Suruga-ku, Shizuoka, Shizuoka 422−8526, Japan
[2]Yokogawa Electric Corporation, 2−9−32 Nakacho, Musashino, Tokyo 180−8750, Japan
[3]Central Research Institute, ITO EN, Ltd., 21 Mekami, Makinohara, Shizuoka 421−0516, Japan
[4]Department of Radiation Life Sciences, Fukushima Medical University School of Medicine, 1 Hikarigaoka, Fukushima, Fukushima 960−1295, Japan
[5]Faculty of Pharmacy, Meijo University, 150 Yagotoyama, Tempaku-ku, Nagoya, Aichi 468−8503, Japan

Abstract Direct nanoelectrospray ionization mass spectrometry (nanoESI-MS) is extremely useful for single-cell analysis to detect endogenous metabolites as well as exogenous compounds that have been taken up. However, during ionization, coexisting constituents, especially sodium chloride, can cause severe matrix effects, resulting in decreased detection sensitivity and fluctuating peak intensities for the compounds of interest. Herein, conventional ESI and nanoESI were examined to determine the extent of ionization suppression by salts using amino acids as typical cellular constituents in addition to caffeine and acetaminophen as exogenous compounds. The corresponding isotope-labeled standard compounds were also tested to compensate for fluctuations. All the tested compounds showed significantly decreased ion intensities with both conventional ESI and nanoESI when ionized with high-concentration salt solutions. However, when the nanospray tip with the smallest inner diameter was used for nanoESI, the peak intensities were 2−3 times higher than those obtained using conventional ESI and their peak intensities recovered to 60% compared to the salt-free samples. These findings clearly demonstrate that nanoESI has advantages over conventional ESI in terms of reducing ionization suppression effects for small molecules in biological samples such as cells containing inorganic salts, particularly sodium chloride, at high concentrations. Furthermore, the use of stable isotope-labeled compounds corresponding to each analyte was revealed to allow adequate correction of the ion peak intensity fluctuations for each analyte during direct nanoESI-MS analysis of single HepG2 cell samples, even when coexisting salts cause severe ion suppression.

Key words: single-cell analysis, direct infusion mass spectrometry, nanoelectrospray ionization, matrix effect, amino acid

Introduction

Live single-cell MS was previously developed by our research group for the rapid analysis of cellular phenomena. In this method, the cellular components in a single living cell were captured into a metal-coated glass capillary under a microscope, and the extracted cellular molecules were directly analyzed by nano electrospray (nanoESI)-MS[1)]. Using direct nanoESI-MS, it has become possible to detect trace samples at the single-cell level without sample loss through absorption by an LC column. This method has been successfully used to develop various applications such as intracellular organelle metabolism analysis[1)], drug subcellular localization analysis[2−4)], and plant cell analysis[5−8)].

*Corresponding author
Hajime Mizuno
Faculty of Pharmacy, Meijo University, 150 Yagotoyama, Tempaku-ku, Nagoya, Aichi 468−8503, Japan
Tel: +81−52−839−2720
E-mail: hmizuno@meijo-u.ac.jp
Received: January 31, 2023. Accepted: February 21, 2023.
Epub April 6, 2023.
DOI: 10.24508/mms.2023.06.003

Recently, for high-throughput biomolecule analysis, direct infusion MS without LC separation has been developed using a high-resolution mass spectrometer[9]. Shotgun lipidomics is a direct MS method for analyzing lipid molecules that are extracted from biological samples without LC separation[10]. The use of nanoelectrospray ionization (nanoESI) enables the highly sensitive mass spectrometric detection of trace samples[11]. In addition, data-independent acquisition[12,13] can be used to identify the detected ion peaks. Ion mobility MS can separate lipid ions with similar *m/z* values depending on differences in lipid structure and identify the corresponding peaks[14,15], and can also identify chiral metabolites when combined with chiral derivatization[16].

However, as no chromatographic separation is performed in direct MS, coexisting components in the sample can suppress or enhance the ionization of analytes. This matrix effect, which causes fluctuations in peak intensities between samples and ion suppression, results in reduced detection sensitivity and reproducibility[17,18]. During the direct MS analysis of biological samples, high concentrations of salts such as sodium, potassium, and chloride have a very large influence of ion suppression[19,20]. In our previous study, it was reported that the ionization suppression effect of salt was greater than that of cell extracts and serum in direct nanoESI analysis[4].

In this study, we demonstrated the effects of salts which from medium and cell lysates on metabolite analysis by direct single-cell MS for accurate comparative analysis of metabolites expressed in each cell. To reduce the matrix effect caused by salts, we decreased the inner diameter of nanoESI emitter and introduced normalization by isotope-labeled internal standards. This detailed data on salt effects during direct nanoESI are expected to be useful for improving the sensitivity and reproducibility of direct MS for the analysis of metabolites in single-cell samples. Finally, single-cell mass spectrometry using HepG2 cells was performed to verify the normalization of the data by the internal standard.

Experimental

Materials

Amino acids (L-phenylalanine, L-tryptophan, and L-tyrosine), caffeine, and acetaminophen were purchased from FUJIFILM Wako Pure Chemical Corporation (Osaka, Japan). Citric acid was purchased from Tokyo Chemical Industry Co. (Tokyo, Japan). A metabolomics QC kit containing ^{13}C-labeled metabolites (alanine, leucine, phenylalanine, tryptophan, tyrosine, caffeine, glucose, benzoate, citrate, octanoate, propionate, stearic acid, succinic acid, and sucrose) was purchased from Cambridge Isotope Laboratories (Tewksbury, MA, USA). Lyophilized human serum was purchased from Nihon Pharmaceutical (Tokyo, Japan). LC/MS-grade methanol was purchased from Kanto Chemical Co. (Tokyo, Japan). LC/MS-grade acetonitrile, formic acid, and ammonium acetate (Optima LC/MS) were purchased from Fisher Scientific (Waltham, MA, USA). All other reagents and solvents were of analytical reagent grade. Water was purified using a PURELAB flex ultrapure water purification system (ELGA LabWater, High Wycombe, UK).

Sample Preparation

High-concentration salt-spiked samples

In this study, amino acids were used as endogenous metabolites, and caffeine was used as an exogenous substance model, respectively. For each analyte, stock solutions with various concentrations (10 μm, 1 μm, 100 nM, and 10 nM) were prepared in saline (154 mmol/L NaCl solution). Each stock solution was further diluted 10 times with 80% methanol containing 0.1% formic acid to obtain concentrations of 1 μm, 100 nM, 10 nM, and 1 nM. The final NaCl concentration of each sample was 15.4 mmol/L. The ^{13}C-labeled internal standards from the metabolomics QC kit were added to the final samples at a concentration of 1 μm. Samples containing other salts (154 mmol/L KCl, 154 mmol/L LiCl, and 154 mmol/L NaH_2PO_4) were prepared in the same way. The control samples were prepared by dissolution in water with no added salts.

Cultured cells and sample collection

The human hepatoma cell line (HepG2, JCRB Cell Bank, Osaka, Japan) was incubated in a CO_2 incubator (5% CO_2, 37°C) with Dulbecco's modified Eagle's medium (FUJIFILM Wako Pure Chemical Corporation, Osaka, Japan) supplemented with 10% fetal bovine serum (biosera, EU origin, FUJIFILM Wako Pure Chemical Corporation, Osaka, Japan), 1% of Gibco 100 × MEM non-essential amino acids (Life Technologies Corp., Gland Island, NY, USA), and 1% of Gibco 100 × Antibiotic-Antimycotic (Life Technologies Corp., Gland Island, NY, USA). Before sampling, the cells were washed three times with PBS (−) (Nacalai tesque, Kyoto, Japan) and the medium was exchanged with PBS

(−). The HepG2 cells were observed with an inverted fluorescence microscope (IX81, Olympus, Japan). The cytoplasm of the target cells was directly micro-sucked into a nanospray tip (Cellomics Tip CT-1, 3 μm of tip inter diameter, HUMANIX, Japan) with a micro-manipulator (MHW-3, Narishige, Japan) operation, respectively. After sampling, 3 μL of ionization solvent (80% methanol containing with 0.1% formic acid and metabolomic QC kit solution) was added into the nanospray tip from the back of the tip.

MS Conditions

nanoESI high resolution MS for salt spiked sample

A 3 μL salt spiked sample was added to the metal-coated glass capillary nanoelectrospray tips (Cellomics Tip CT-1 (tip approximate bore size: 3 μm), and Cellomics Tip CT-10 (tip approximate bore size: 10 μm), HUMANIX, Hiroshima, Japan), and the tip was set on a nanoESI ion source. Full scan mass spectrometric detection was performed on a Q-TOF mass spectrometer (Xevo G2-XS Q-Tof, Waters, Milford, MA, USA). The spray voltages for positive and negative ion detection were 1.0 kV and −0.8 kV, respectively. The mass spectrometric conditions were as follows: cone voltage, 20 V; source temperature, 100°C; cone gas flow, 0 L/h; nano flow gas, 0.20 bar; purge gas flow, 350 L/h; mass range, *m/z* 70−1,000; analyzer mode, sensitive; scan time, 0.5 s/scan; data format, continuum; acquisition time, 3.0 min. The mass spectrometer was calibrated before analysis using a calibration solution containing sodium formate.

nanoESI QQQ MS for salt spiked sample

A 3 μL salt spiked sample was added to the nanoelectrospray tip, and the tip was set on a nanoESI ion source. Selected reaction monitoring (SRM) detection was performed on a QQQ mass spectrometer (Xevo TQ-S micro, Waters, Milford, MA, USA). The spray voltage was set at 1.0 kV for positive ion detection. The mass spectrometric conditions were as follows: cone voltage, 20 V; source temperature, 100°C; cone gas flow, 0 L/h; nano flow gas, 0.20 bar; purge gas flow, 350 L/h; data format, continuum; acquisition time, 3.0 min. The SRM transitions of the analytes are shown in Table 1.

NanoESI high resolution MS for single-cell sample

For single-cell analysis, we used a high-resolution mass spectrometer (Orbitrap Fusion Lumos Tribrid equipped with a nanoESI source, Thermo Fisher Scientific, MA, USA). The mass spectrometric conditions were as follows: maximum injection time, 100 ms; mass resolution, 120,000 at *m/z* 400; scan range, *m/z* 100−700; ion transfer tube temperature, 200°C; ion spray voltage, 1000 V for positive ion mode.

Table 1. SRM transitions of analytes and their isotope-labeled internal standards

Compound	Q1 (*m/z*)	Q3 (*m/z*)	Collision energy (V)
Leucine	132.1	86.1	25
^{13}C- Leucine	138.1	91.1	
Phenylalanine	166.1	120.1	25
^{13}C-Phenylalanine	1372.1	126.1	
Tyrosine	182.1	136.1	25
^{13}C-Tyrosine	188.1	142.1	
Tryptophan	205.1	146.1	30
^{13}C-Tryptophan	216.1	153.0	
Acetaminophen	152.1	110.1	35
Caffeine	195.1	138.1	30

Data Analysis

The MS data were evaluated using the MassLynx (Waters, Milford, MA, USA) and the Xcalibur (Thermo Fisher Scientific, MA, USA) software and exported to a peak list. Peak alignment for the peak list of each sample list was performed using the MarkerView software (Sciex, Framingham, MA, USA). Statistical analysis and calibration curve preparation for each substance were performed using Excel (Microsoft).

Results and Discussion

Analysis of high salt samples by direct nanoESI-MS

To demonstrate ion suppression effects by salts, standard samples of the analytes (1 μm in 15.4 mM NaCl) were analyzed by direct infusion nanoESI high resolution MS using 3 μL of the sample solution in a nanoESI tip (tip i.d. 3 μm).

Fig. 1 shows the high resolution full scan mass spectra of standard samples with and without salt (NaCl and KCl) at the same concentration. In the expanded spectra of each analyte (phenylalanine, tyrosine, tryptophan, and caffeine), the peak intensities of them in the sample decreased with salt addition. In the LiCl-spiked sample, none of the ion peaks of these analytes were detected.

Fig. 2(a)−(d) show the average peak intensities (n=3) of

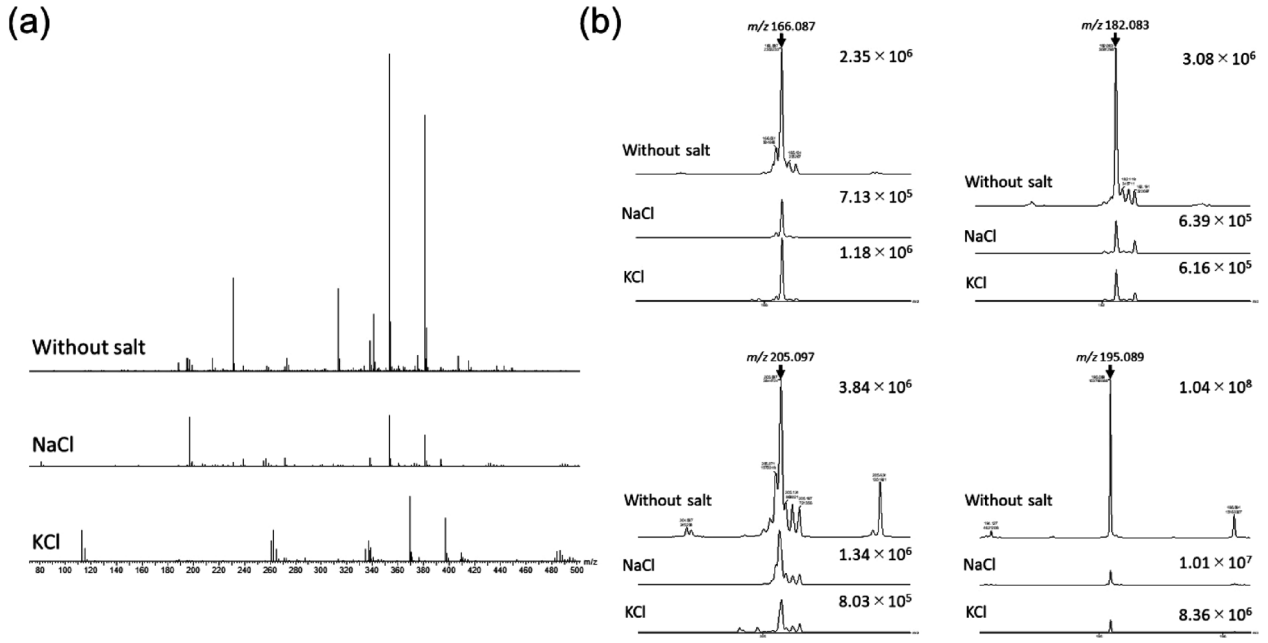

Fig. 1. (a): Full scan direct nanoESI mass spectra of standard samples with NaCl (middle spectrum) and KCl (lower spectrum) and control (without salt) samples (upper spectrum). (b): The expanded mass spectra of (a), amino acids (Phe, Tyr, and Trp), and caffeine.

The protonated ion peak of each standard is indicated by the arrowhead. The intensity of each ion peak is shown on the upper right of each spectrum.

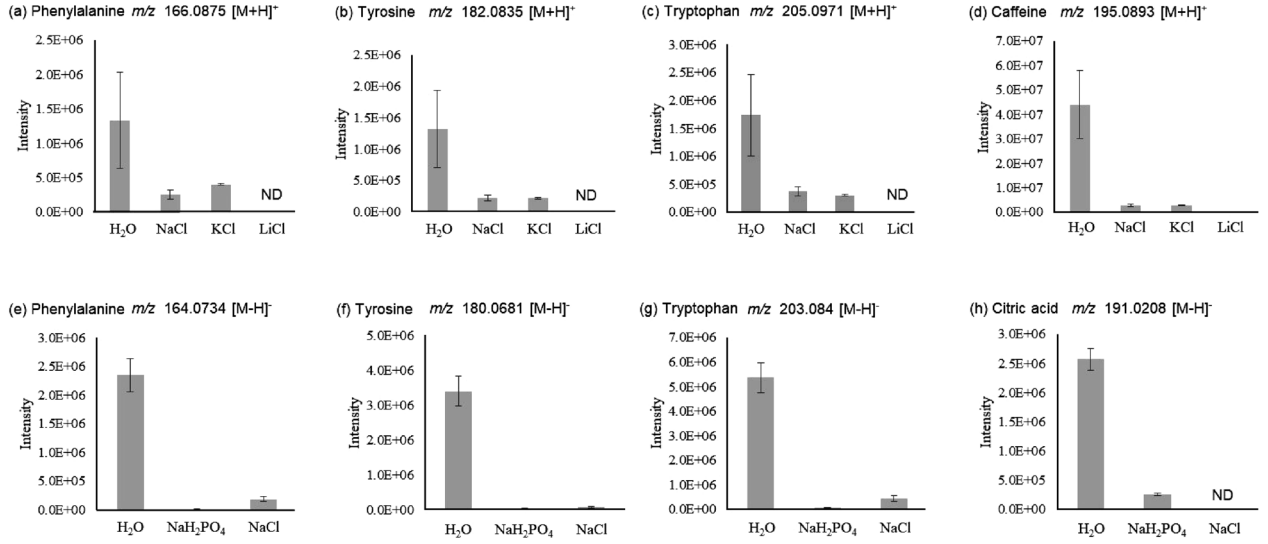

Fig. 2. Averaged peak intensities of compounds in each salt spiked sample.

(a)−(d) are detected by the positive ion mode. (e)−(h) are detected by negative ion mode.

the analyte ions in various salt solutions detected in the positive ion mode. All the ion peaks were significantly reduced in the salt-spiked samples (NaCl, KCl, and LiCl) compared with those in the samples without salt. This result shows that high concentrations of metal ions other than sodium ions in the sample have similar ionization suppression effects[21]. The ion suppression effects decreased in the order $Li^+ > Na^+ > K^+$, suggesting an association with ionization tendency.

Na^+-adduct peaks were detected for both phenylalanine and tryptophan in the salt-spiked and control samples. In the LiCl- and KCl-spiked samples, $Li^+$and K^+adduct ion peaks were not detected for phenylalanine and tryptophan, but Na^+adduct ion peaks were still observed. Thus, these Na^+adduct ion peaks may be the result of Na^+eluted from the borosilicate glass surfaces of the solvent stock bottles

and the nanoESI glass capillaries. In the NaCl-spiked samples, the intensities of the Na^+adduct ion peaks of these amino acids decreased, similar to the above-described behavior for caffeine. These results show that the addition of a high salt concentration effectively suppresses positive ESI.

In the negative ion detection mode, compounds such as amino acids and citric acid were detected as deprotonated ion peaks (Fig. 2(e)−(h)). Almost no analyte ion peaks were detected in samples spiked with sodium chloride or sodium dihydrogen phosphate.

These results show that the ion suppression effect of high salt concentrations was more significant in the negative ion mode than in the positive ion mode, regardless of chloride or phosphate ions. Thus, when using MS to analyze biological samples containing high concentrations of saline, the detection sensitivity is significantly lowered by the ion suppression effect of ESI.

On the other hand, for all the ESI methods, the peak intensities were improved by 10 times dilution of the salt concentration. Table 2 shows the limit of detection (LOD) values for analytes in the presence and absence of NaCl. Compared with the control samples, the samples spiked with high concentrations of NaCl showed a 5−25-fold decreased in sensitivity for most analytes. In contrast, when the salt concentration was diluted 10 times, the sensitivity only showed a 2.5-fold decrease. Thus, the salt concentration in the sample greatly affects ion suppression.

For our single-cell MS, sampling volumes from single-cells range from several hundreds of fL to a few tens of pL. Then, 2 μL of ionized solvent is added to the nanoESI tip to extract cellular components. Therefore, diluted single-cell samples are expected to be less affected by the ion suppression effect. In the case of single-cell MS, the sampling volume from a cell is between 100 fL to 20 pL. Then, 2 μL of ionization solvent is added to the nanoESI tip. The reason why ion suppression effects were decreased in diluted single-cell sample.

Table 2. The LOD of nanoESI-MS analysis using CT-1 nanospray tip for each standard compound in high and low NaCl spiked samples

	LOD[a] (nmol/L)		
	H_2O	NaCl	1/10 NaCl
Phenylalanine	10	250	25
Tyrosine	100	500	250
Tryptophan	100	500	250
Caffeine	10	250	25

[a]: The peaks above s/n>3.0 were used for LOD calculation.

Comparison of ion suppression ratios with nanoESI and conventional ESI

Next, the influence or the size of the nanoESI tip top and the ionization suppression effect of salt were investigated. To evaluate the ion suppression effect in each sample, Equation 1 was used to calculate the extent by which the addition of salt reduced the peak intensity as compared to the unsalted control sample.

$$\text{Relative intensity}(\%) = \frac{\text{Intensity}\left(\text{Salt-spiked sample}\right)}{\text{Intensity}\left(\text{Control}\right)} \times 100 \quad (1)$$

Fig. 3 shows the peak suppression ratio of each compound (250 nM) for each ESI method with SRM positive ion detection by QQQ mass spectrometer. Although ion suppression effects were also observed for the nanoESI results in the presence of various salts, the suppressed relative intensity ratios were bigger than those for conventional ESI. The ion suppression effect for each ESI method is considered to be related to the inner diameter of the capillary used during ionization. The inner diameters of the conventional ESI capillary and the nanoESI tips were 127 μm, 3 μm, and 10 μm, respectively. In the high-concentration NaCl samples, the peak intensities of most analytes were 20% or less of those in the control samples, indicating a large ion suppression effect. Nevertheless, nanoESI with the 3 μm i.d. tip provided improved peak intensities as compared to conventional ESI and nanoESI with the 10 μm i.d. tip. In particular, in the 10 times diluted NaCl samples, the peak suppression ratios with the 3 μm i.d. tip were 2−3 times higher than those with conventional ESI. As a result, the peak intensities were recovered to approximately 60% of those for the samples without NaCl. In the case of the 10 μm i.d. tip, the peak suppression ratios were similar to those for conventional ESI. These results indicate that the 3 μm i.d. tip, which is the nanospray tip with the smallest inner diameter, minimizes the effect of ion suppression by NaCl.

Next, the relationship between these inner diameters and the sample flow rate was investigated. For nanoESI using the 3 μm and 10 μm i.d. tips, off-line infusion with no back pressure was used, and sample solution spraying and ionization were automatically performed by applying a voltage. The flow rate of each emitter was determined by measur-

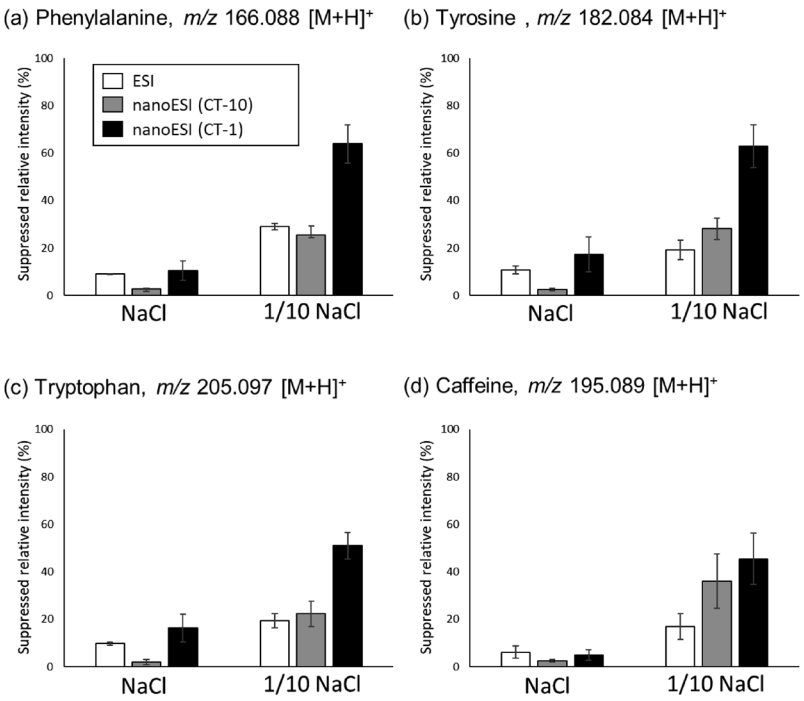

Fig. 3. Suppression rate of each substance ion peak (a): phenylalanine, (b): tyrosine, (c): tryptophan, and (d): caffeine high-concentration NaCl (15.4 mM) and 10-fold diluted NaCl-spiked samples.
The bar graphs colored white show the results of ionization with conventional ESI. Similarly, the gray and black bars indicate the CT-10 and CT-1 nanospray tip, respectively.

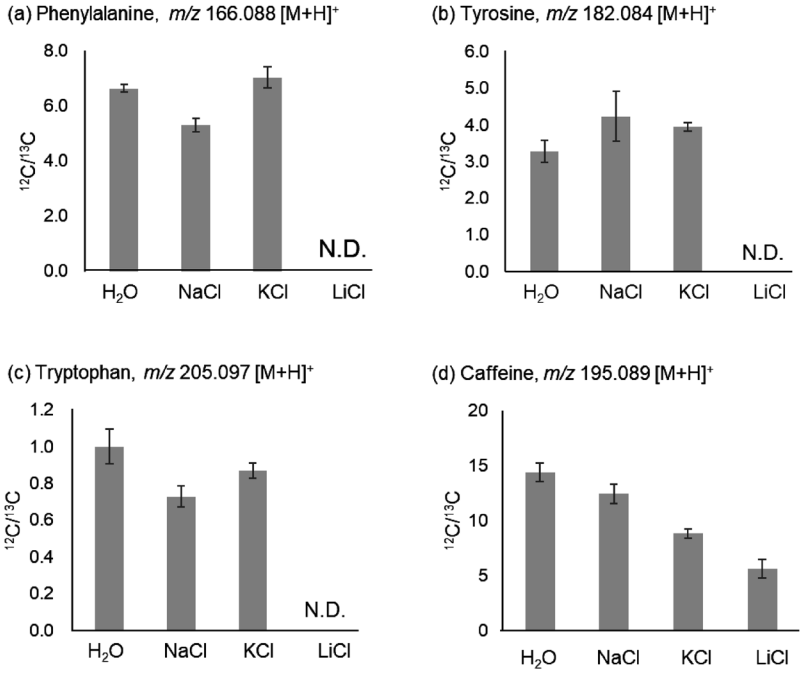

Fig. 4. Averaged peak intensities of compounds (Phenylalanine (a), Tyrosine (b), Tryptophan (c), and Caffeine (d)) which were normalized with internal standard (^{13}C labeled I.S.) in each salt spiked sample (0.9% each).
(a)−(d) are detected by the positive ion mode. (e)−(h) are detected by negative ion mode.
Averaged peak intensities which were normalized with each ^{13}C labeled substance. Normalized ion peaks of each substance in high salt concentration samples (15.4 mM each).

ing the time at which no further ions from the sample were detected by the mass spectrometer. The flow rates of the 3 μm and 10 μm i.d. emitters were 68±9.5. and 180±57 nL/min, respectively. Compared with conventional ESI (flow rate: 100 μL/min), nanoESI is quite slow.

These results demonstrate that the influence of ion suppression can be reduced, even in samples with high salt concentrations, by using a capillary with a small tip diameter and a low sample flow rate during ionization. Previous studies have reported that lower sample flow rates and smaller tip inner diameters reduce the size of the charged droplets in the nanoESI spraying process[22,23]. As the rate of droplet evaporation increases with decreasing droplet size, smaller charged droplets can easily reach the Rayleigh limit. In addition, these initial droplets are expected to have a low salt concentration owing to an abundance of protons resulting from the exclusion-enrichment effect (EEE), which releases protons from the silanols on the inner surface of the nanospray tip[21].

Normalization by internal standards

To account for fluctuations and the reduction in peak intensity caused by ion suppression, stable isotope-labeled substances (^{13}C-labeled phenylalanine, tryptophan, tyrosine, and caffeine) were added to the samples as internal standards. The stable isotope dilution method, in which a compound labeled with a stable isotope (^{13}C, ^{2}H, ^{15}N, etc.) is used as an internal standard, is a useful normalization method for quantitative analysis using MS[24,25]. The ionization efficiencies of the ^{13}C-labeled internal standards used in this study were the same as those of the unlabeled forms with both nanoESI and conventional ESI.

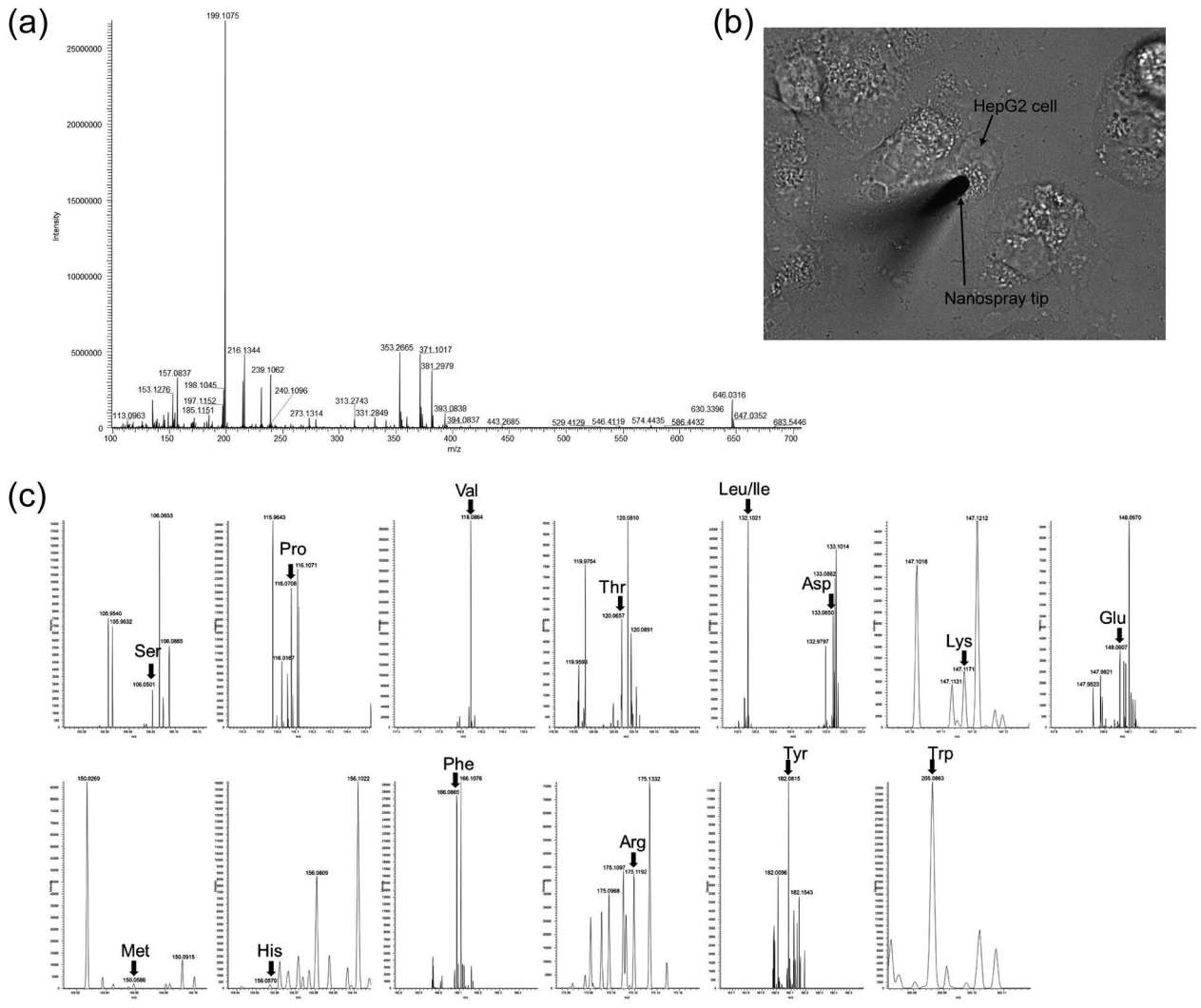

Fig. 5. The full scan mass spectrum of a single HepG2 cytoplasm (a). The microscope capture of HepG2 cytoplasm sampling (b). Each amino acid mass spectrum (c) which is expanded from (a).
The peaks indicated by arrows are protonated amino acid ions.

Table 3. The peaks of amino acid ions detected in a single HepG2 cytoplasm sample (n=6), their average intensity, standard deviation, and CV values, and the CV values after normalization with internal standard peaks

Amino acid	*m/z*	Averaged intensity	SD	CV (%)	Normalized CV (%)	IS peak
Leucine/Isoleucine	132.1022	66745	32315	48	**32**	^{13}C-Leu
Phenylalanine	166.0866	31203	16858	54	**29**	^{13}C-Phe
Tyrosine	182.0815	17835	10495	59	**37**	^{13}C-Tyr
Tryptophan	205.0976	2833	2674	94	**81**	^{13}C-Trp
Serine	106.0501	5565	2724	49	**26**	^{13}C-Phe
Threonine	120.0656	10721	5933	55	**34**	^{13}C-Phe
Asparagine	133.061	169	110	65	**40**	^{13}C-Phe
Glutamate	148.0607	5045	2262	45	**35**	^{13}C-Phe
Proline	116.0708	27877	5756	21	**26**	^{13}C-Phe
Valine	118.0865	37701	24016	64	**67**	^{13}C-Phe
Lysine	147.1131	21359	28857	135	**114**	^{13}C-Phe
Methionine	150.0586	4840	4029	83	**71**	^{13}C-Phe
Histidine	156.0771	5579	9171	164	**150**	^{13}C-Phe
Arginine	175.1193	26076	31813	122	**104**	^{13}C-Phe

Fig. 4 shows the normalized results for the ion peak of each analyte in control sample and salt-spiked (NaCl, KCl, and LiCl) samples. In the salt-spiked samples, the peak intensities of most analytes decreased significantly, as shown in Fig. 2. However, after normalization by the corresponding stable isotope-labeled internal standards, the peak intensities were improved to almost the same level as those in the unsalted control samples. Moreover, the fluctuations in the peak intensities were also improved. These results indicate that normalization with the stable isotope-labeled ion peak for each analyte adequately corrects for ion suppression in the salt-containing samples and peak intensity fluctuations between samples.

Furthermore, we investigated whether this normalization method could be applied using a stable isotope-labeled internal standard and analyte with different structures. Normalization of the caffeine ion peaks spiked using the ion peaks of ^{13}C-labeled tyrosine provided no improvement in peak intensity, as shown in Fig. 4(d). However, the sample-to-sample fluctuation (CV values) of the caffeine ion peak improved from 15−55% to 8.6−26% (data not shown). In this case, it was difficult to completely normalize the ion suppression and ionization efficiency because of the differences in the physical properties of the amino acid internal standard and the analyte. However, as this normalization procedure improved peak fluctuation, it could to be useful for comparative analyses of samples. Furthermore, if a more detailed analysis of multiple metabolites is required, our previously developed universal normalization method using stable isotope-labeled algal cell extracts as multiple internal standards[24] could be applied.

Application for Single-cell analysis

Next, this method was applied to single-cell MS. The cytoplasm of human hepatoma cells (HepG2 cells) was captured into a nanospray tip under microscopic observation. In this study, we used a 3 μm i.d. nanospray tip which is a suitable sampling of intracellular cytoplasm components. Then, 3 μL of solution extracted with 80% methanol containing 0.1% formic acid and metabolomic QC kit solution was added to the nanospray tip for nanoESI-Orbitrap MS analysis in positive ion detection mode.

Fig. 5 shows the single-cell full scan (Fig. 5(a)) and focused mass spectra to each amino acid ion peak (Fig. 5(c)) from single HepG2 cytoplasm sample. The microscope capture image of a HepG2 cell sampling by nanospray tip is shown in Fig. 5(b). Although intensities of the detected peaks were very small due to a single cell sample, the m/z values of these peaks were close to the theoretical values for amino acids within a mass error of +/− 5 ppm. These peaks were not detected in the blank samples in which the cell culture medium (PBS) were sampled. From the results, these peaks were annotated amino acids derived from single-cell.

Table 3 shows the ion peaks of the amino acids detected in the cytoplasm of a single HepG2 cell (n=6) as well as their average intensities, standard deviations, coefficient of variation (CV) values, and CV values after normalization

by internal standards. The Leu, Phe, and Tyr ion peaks were normalized using the corresponding stable isotope ion peaks in the metabolomics QC kit, and the CV values were significantly improved. The ion peaks of the other amino acids were normalized by the stable isotope-labeled Phe peak, which also improved the CV values. However, the effect of normalization for low-intensity ion peaks (＜5,000) such as Asn, Trp, and Met was small, due to the detection sensitivity of the mass spectrometer. Some amino acids showed high CV values despite having high peak intensities. Since essential amino acids are consumed in large amounts during cell proliferation of cancer cells such as HepG2, intracellular amino acid expression levels vary depending on cell conditions[25]. On the other hand, Arginine is a non-essential amino acid, but it is rapidly metabolized to urea and ornithine in the urea cycle. In particular, since cancer cells proliferate rapidly, it is thought that the amount of arginine in the cytoplasm varies depending on the cells[26].

Conclusion

In this study, the matrix effects due to salt and intracellular components in single-cell mass spectrometry using direct nanoESI were examined. As a result, it was confirmed that the effect of salt on nanoESI ionization can be suppressed by reducing the tip diameter of the nanoelectrospray tip and diluting the sample. Furthermore, by using the stable isotope-labeled metabolites of amino acids as the internal standards, good normalization of amino acids and other metabolites was achieved. These methods were applied to single-cell MS to analyze amino acids in the cytoplasm of HepG2 cells, and fluctuations in amino acid peaks due to matrix effects were suppressed. From this, it was confirmed that quantitative analysis of metabolites that detect high peak intensities is possible by suppressing the influence of matrix effects by direct nanoESI mass spectrometry.

In the future, we aim to develop this method that can detect various intracellular metabolites with more sensitive and elucidate cellular phenomena at the molecular level.

Author Contributions

Y. Kato and H. Mizuno performed the experiments and analyzed the data. H. Mizuno, S. Kudoh, and N. Tsuyama contributed to experimental design. E. Sugiyama and I. Sakane contributed to analyzing data. T. Toyo'oka and K. Todoroki supervised this work. The manuscript was written by H. Mizuno in collaboration with the other authors. All authors have approved the final version of the manuscript.

Acknowledgements

The authors are grateful to Dr. Kentaro Takahara, Dr. Daisuke Higo, and Mr. Masanori Fukushima (Thermo Fisher Scientific K.K., Japan) for performing single-cell MS analysis. This study was supported in part by a Grant-in-Aid for Scientific Research (19K07028) from the Ministry of Education, Culture, Sports, Science, and Technology of Japan (H.M.).

Conflicts of Interest

There are no conflicts to declare.

References

1) Mizuno H, Tsuyama N, Harada T, Masujima T: Live single-cell video-mass spectrometry for cellular and subcellular molecular detection and cell classification. *J Mass Spectrom* 43: 1692−1700, 2008.
2) Date S, Mizuno H, Tsuyama N, Harada T, Masujima T: Direct drug metabolism monitoring in a live single hepatic cell by video mass spectrometry. *Anal Sci* 28: 201−203, 2012.
3) Fukano Y, Tsuyama N, Mizuno H, Date S, Takano M, et al: Drug metabolite heterogeneity in cultured single cells profiled by pico-trapping direct mass spectrometry. *Nanomedicine* 7: 1365−1374, 2012.
4) Yahata K, Mizuno H, Sugiyama E, Todoroki K: Analysis of the intracellular localization of amiodarone using live single-cell mass spectrometry. *J Pharm Biomed Anal* 205: 114318, 2021.
5) Lorenzo Tejedor M, Mizuno H, Tsuyama N, Harada T, Masujima T: In situ molecular analysis of plant tissues by live single-cell mass spectrometry. *Anal Chem.* 84: 5221−5228, 2012.
6) Fujii T, Matsuda S, Lorenzo Tejedor M, Esaki T, Sakane I, et al: Direct metabolomics for plant cells by live single-cell mass spectrometry. *Nat Protoc* 10: 1445−1456, 2015.
7) Yamamoto K, Takahashi K, Mizuno H, Anegawa A, Ishizaki K, et al: Cell-specific localization of alkaloids in Catharanthus roseus stem tissue measured with imaging MS and single-cell MS. *Proc Natl Acad Sci USA* 113: 113, 3891−3896, 2016.

8) Shimizu T, Miyakawa S, Esaki T, Mizuno H, Masujima T, et al: Live single-cell plant hormone analysis by video-mass spectrometry. *Plant Cell Physiol* 56: 1287−1296, 2015.
9) Pöhö P, Lipponen K, Bespalov MM, Sikanen T, Kotiaho T, et al: Comparison of liquid chromatography-mass spectrometry and direct infusion microchip electrospray ionization mass spectrometry in global metabolomics of cell samples. *Eur J Pharm Sci* 138, 104991, 2019.
10) Hsu F-F: Mass spectrometry-based shotgun lipidomics—A critical review from the technical point of view. *Anal Bioanal Chem* 410: 6387−6409, 2018.
11) Juraschek R, Dülcks T, Karas M: Nanoelectrospray—More than just a minimized-flow electrospray ionization source. *J Am Soc Mass Spectrom* 10: 300−308, 1999.
12) Gethings LA, Richardson K, Wildgoose J, Lennon S, Jarvis S, et al: Lipid profiling of complex biological mixtures by liquid chromatography/mass spectrometry using a novel scanning quadrupole data-independent acquisition strategy. *Rapid Commun Mass Spectrom* 31: 1599−1606, 2017.
13) Gao F, McDaniel J, Chen EY, Rockwell HE, Nguyen C, et al: Adapted MS/MSALL shotgun lipidomics approach for analysis of cardiolipin molecular species. *Lipids* 53: 133−142, 2018.
14) Shvartsburg AA, Isaac G, Leveque N, Smith RD, Metz TO: Separation and classification of lipids using differential ion mobility spectrometry. *J Am Soc Mass Spectrom* 22: 1146−1155, 2011.
15) Paglia G, Kliman M, Claude E, Geromanos S, Astarita G: Applications of ion-mobility mass spectrometry for lipid analysis. *Anal Bioanal Chem* 407: 4995−5007, 2015.
16) Fukui S, Sugiyama E, Mizuno H, Sakane I, Asakawa D, et al: Rapid chiral discrimination of oncometabolite dl-2-hydroxyglutaric acid using derivatization and field asymmetric waveform ion mobility spectrometry/mass spectrometry. *J Sep Sci* 44: 3489−3496, 2021.
17) Rossmann J, Gurke R, Renner LD, Oertel R, Kirch W: Evaluation of the matrix effect of different sample matrices for 33 pharmaceuticals by post-column infusion. *J Chromatogr B* 1000: 84−94, 2015.
18) Stahnke H, Kittlaus S, Kempe G, Hemmerling C, Alder L: The influence of electrospray ion source design on matrix effects. *J Mass Spectrom* 47: 875−884, 2012.
19) Iavarone AT, Udekwu OA, Williams ER: Buffer loading for counteracting metal salt-induced signal suppression in electrospray ionization. *Anal Chem* 76: 3944−3950, 2004.
20) Metwally H, McAllister RG, Konermann L: Exploring the mechanism of salt-induced signal suppression in protein electrospray mass spectrometry using experiments and molecular dynamics simulations. *Anal Chem* 87: 2434−2442, 2015.
21) Hu J, Guan Q-Y, Wang J, Jiang X-X, Wu Z-Q, et al: Effect of nanoemitters on suppressing the formation of metal adduct ions in electrospray ionization mass spectrometry. *Anal Chem* 89: 1838−1845, 2017.
22) Schmidt A, Karas M, Dülcks T: Effect of different solution flow rates on analyte ion signals in nano-ESI MS, or: When does ESI turn into nano-ESI? *J. Am Soc Mass Spectrom* 14: 492−500, 2003.
23) Wilm M, Mann M: Analytical properties of the nanoelectrospray ion source. *Anal Chem* 68: 1−8, 1996.
24) Mizuno H, Ueda K, Kobayashi Y, Tsuyama N, Todoroki K, et al: The great importance of normalization of LC-MS data for highly-accurate non-targeted metabolomics. Biomed Chromatogr 31: e3864, 2017.
25) Weindl D, Wegner A, Jäger C, Hiller K: Isotopologue ratio normalization for non-targeted metabolomics. *J Chromatogr A* 1389: 112−119, 2015.
26) Nilsson A, Haanstra JR, Engqvist M, Gerding A, Bakker BM, et al: Quantitative analysis of amino acid metabolism in liver cancer links glutamate excretion to nucleotide synthesis. *Proc Natl Acad Sci USA* 117: 10294−10304, 2020.
27) Zou S, Wang X, Liu P, Ke C, Xu S: Arginine metabolism and deprivation in cancer therapy. *Biomed Pharmacother* 118: 109210, 2019.